Tectonophysics 606 (2013) 178–186

Contents lists available at ScienceDirect

Tectonophysics

journal homepage: www.elsevier.com/locate/tecto

Normal faulting from simple shear rifting in South Tibet, using evidence from passive seismic profiling across the Yadong-Gulu Rift

Zhongjie Zhang [a,*], Yun Chen [a], Xiaohui Yuan [b], Xiaobo Tian [a], Simon L. Klemperer [c], Tao Xu [a], Zhiming Bai [a], Hongshuang Zhang [a], Jing Wu [a], Jiwen Teng [a]

[a] State Key Laboratory of Lithospheric Evolution, Institute of Geology and Geophysics, Chinese Academy of Sciences, Beijing, 100029, China
[b] Deutsches GeoForschungsZentrum GFZ, Telegrafenberg, 14473 Potsdam, Germany
[c] Department of Geophysics, Stanford University, Stanford, CA 94305, USA

ARTICLE INFO

Article history:
Received 10 September 2012
Received in revised form 4 March 2013
Accepted 14 March 2013
Available online 22 March 2013

Keywords:
Normal fault
South Tibet
Passive source seismic profiling
Simple shear rifting

ABSTRACT

The Tibetan Plateau is undergoing north–south shortening accompanied by west–east extension, as evidenced by the widespread development of north–south trending normal faults, grabens and rifts. While the mode of the north–south shortening has been the main focus of most international studies, knowledge of the deep structure beneath South Tibet is required for understanding the mechanism of the west–east extension. The onset of the north–south trending normal faulting is commonly taken as an indicator that the Tibetan Plateau was uplifted to a near-maximum elevation before entering a collapsing stage. Here we report on the receiver functions of a seismological experiment across the northern segment of the Yadong-Gulu Rift (YGR), one of the youngest rifts in South Tibet. The migrated receiver function images reveal that the YGR is a high-angle normal fault characterized by a 5-km Moho rise from its western to eastern flank, together with distinct differences in the crustal structure and intracrustal seismic conversion patterns between the two flanks. This highly asymmetric lithospheric structure suggests whole-crustal extension controlled by a simple/general shear rifting mechanism. This simple/general shear rifting in the YGR is attributed to an eastward (horizontal) shear at the base of the upper crust, as evidenced by the observed Tibetan GPS velocity field and our observation of shear wave splitting discrepancy among the upper crust, lower crust and lithospheric mantle. We propose that in the YGR, simple shear rifting accommodates the northward injection of the Indian lithosphere, which may suggest that the onset of the north–south normal faulting does not indicate gravitational collapse of the Tibetan lithosphere.

1. Introduction

The formation of the Tibetan Plateau is commonly accepted to have resulted from convergence and collision between the Indian and Eurasian plates, beginning 50 Ma ago (Yin and Harrison, 2000). During the Indo-Asian collision, India penetrated more than 1500 km northward, and there is a considerable debate about how such a great amount of crustal shortening has been accommodated. Different geodynamic processes such as crustal thickening, tectonic escaping, lower crustal flow, normal faulting and others have been proposed, with constraints from tectonic, surface geology, physical and numerical modeling studies. A crustal thickening model suggests that the collision of India into Asia has been accommodated by the distributed north–south shortening (Dewey and Burke, 1973). The lateral extrusion hypothesis emphasizes the role of large-scale strike-slip faults in transporting relatively undeformed continental blocks eastwards, away from the Indo-Asian convergent front (Peltzer and Tapponnier, 1988). Normal faulting (Yin and Harrison, 2000) has absorbed the north–south shortening by tens of kilometers. The onset of the north–south trending rifts has also been considered to indicate that the plateau, with an average altitude of >4000 m, reached its maximum elevation and entered into lithospheric collapse (e.g., Armijo et al., 1986). It would be useful to clarify the deep structure of the normal faulting in order to understand the mechanisms at work during the continental collision.

The widespread development of the north–south trending rifts (roughly perpendicular to the India-Eurasia convergence direction) is commonly attributed to the east–west extension of southern Tibet (Larson et al., 1999). Several mechanisms have been proposed for these rifts to explain the mode of the west–east extension. These include: (1) orogenic collapse (Kapp et al., 2008; Liu and Yang, 2003), (2) middle/lower crustal flow (Royden et al., 2008; Shapiro et al., 2004); (3) shearing from a series of west–east trending shear faults (Ratschbacher et al., 2011; Taylor et al., 2003); (4) lithospheric delamination (Houseman and England, 1996); (5) magmatism (Kapp et al., 2005) or (6) lower crustal underplating (Vergne et al., 2008). These models differ in terms of whether the west–east extension is at the crustal or the lithospheric scale, and can be divided into two categories. One type of model supports the Tibetan Plateau attaining

* Corresponding author. Tel.: +86 13701357365.
E-mail address: zjzhang1@yahoo.com (Z. Zhang).

0040-1951/$ – see front matter © 2013 Elsevier B.V. All rights reserved.
http://dx.doi.org/10.1016/j.tecto.2013.03.019

its maximum elevation as part of a gravitational collapse model (Molnar and Tapponnier, 1978; Tapponnier et al., 1981), while others hold that the east–west extension has been accompanied by the north–south shortening, and does not require the plateau to reach a maximum elevation. The second category includes the oblique convergence of the Indian subduction (Kapp and Guynn, 2004; McCaffrey and Nabelek, 1998), shearing from a series of west–east trending shear faults (Ratschbacher et al., 2011; Taylor et al., 2003); lithospheric fragmentation under a particular regional boundary condition throughout East Asia (Yin, 2000), triggering by magmatism (Harrison, 2006), and deformation facilitated by mantle lithospheric delamination (Houseman and England, 1996; Ren and Shen, 2008). In order to evaluate the tectonic models for the north–south trending faulting (or rifting) in central Tibet, we obtained passive-source seismic observations for one year along a profile across the Yadong-Gulu Rift (Fig. 1) and imaged the structure of the crust and upper mantle using the widely used receiver function method (Yuan et al., 1997). The resulting information on the crustal and upper mantle structure across the YGR provides new insights into the origin of the north–south trending rifts.

2. Tectonic setting of the study area

The main Cenozoic structures in southern Tibet include the north–south trending rifts and WNW-trending right slip faults (Fig. 1b) (Armijo et al., 1986, 1989). From west to east in the Lhasa Terrane, the north–south trending normal faults (also called rifts) become younger to the east, with rifting ages of 24 Ma for Tangra Yum Tso, about 23 Ma for Rongqingxiubu Tso, 14 Ma for Shenza and 8 Ma for the Yadong-Gulu Rift (Chung et al., 2005). Information on the rifting ages for the Tibetan Plateau indicates that the YGR is the most significant and the youngest rift, with its central segment having been initiated about 5 to 8 Ma ago (Harrison et al., 1995; Maheo et al., 2007). It has been estimated that YGR has accommodated >20 km of east–west extension (Harrison et al., 1995). It is therefore an excellent natural laboratory for studying the deep process of the north–south trending normal faulting or rifting at the same time as the north–south shortening and convergence between the Indian and Eurasian plates.

The YGR extends nearly north-southwards in its southern part and then to the NNE in its northern part (Fig. 1). As an asymmetrical normal fault system with a width of about 30–40 km, the YGR displays a generally steeper and higher topography on its western than its eastern flank. Many geophysical experiments, such as the first wide-angle seismic profiling in the 1970s by the Chinese Academy of Sciences (Teng et al., 1981), the INDEPTH deep seismic reflection program (Zhao et al., 1993) and the GEDEPTH wideband passive source seismic profiling (Kind et al., 2002; Yuan et al., 1997) have been carried out along the YGR in the last 40 years (Zhang et al., 2011). Crustal and lithospheric-scale geophysical experiments along the YGR (Hirn et al., 1984; Nelson et al., 1996; Owens and Zandt, 1997; Teng et al., 1981; Zhao et al., 1993) have helped our understanding of the deep processes operating at the convergence of the Indian and Eurasian plates along the rift. Our west–east profile across the YGR provides complimentary constraints to help understand the west–east extension and the development of the YGR during this north–south continent–continent convergence and collision.

3. Brief description of seismic data acquisition and receiver function

The passive seismic observation experiment described herein was carried out along a profile across the northern segment of the Yadong-Gulu Rift in the northern Lhasa Terrane (Fig. 1) between September 2009 and November 2010. In this experiment, 11 seismographs were

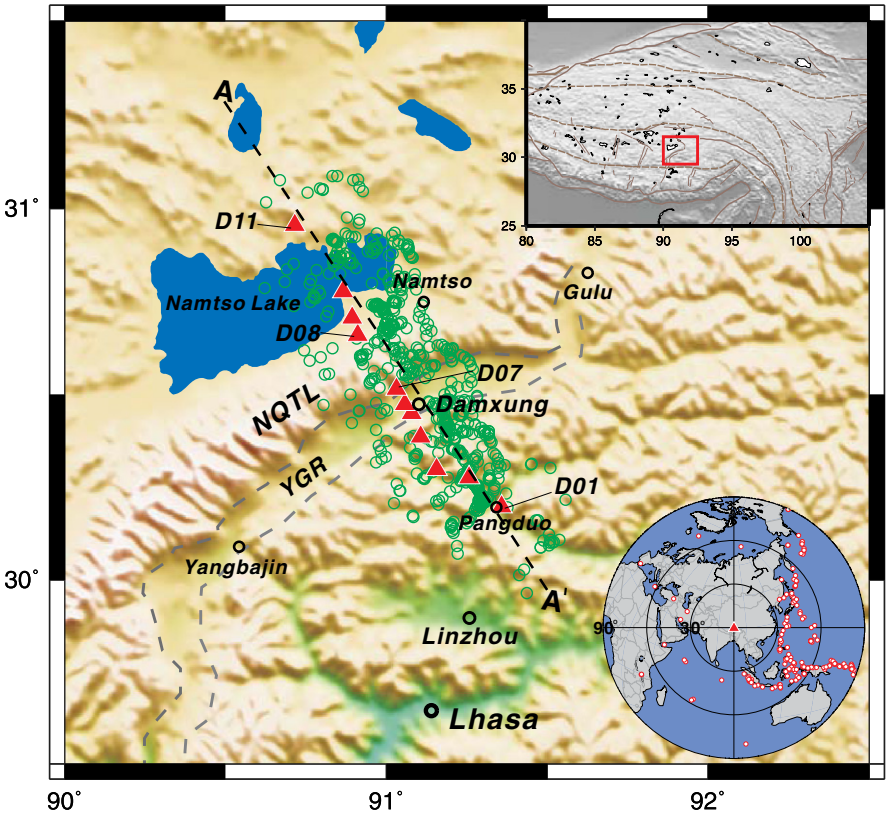

Fig. 1. Tectonic and topographic map of the Yadong-Gulu Rift in the Tibetan Plateau. Red triangles denote seismic stations and green circles show Ps piercing points at the Moho depth (70 km). The upper right inset shows a map of the Tibetan Plateau. The lower right inset shows the teleseismic events used in this study.

deployed. Stations D01–D04 were located in the eastern flank of the YGR, D05–D07 were located at the rift with a station interval of ~5 km, and stations D08–D11 were located on the western flank of the rift.

During the 14-month period of operation, 200 earthquakes with magnitude greater than Ms 5.5 were recorded in the distance range between 30 and 90° (see Fig. 1). We visually selected records with a high signal-to-noise (S/N) ratio for each station and calculated receiver functions using a time-domain iterative deconvolution with vertical and radial seismograms (Kind et al., 2012; Ligorria and Ammon, 1999). Fig. 2a displays the raw P-receiver function grouped for each station. In order to enhance signal/noise ratio of seismic conversions, move-out corrected receiver functions for each station (e.g. Zandt and Ammon, 1995) are stacked as shown in Fig. 2b where the stacks are implemented in 21 windows of PS conversion with window size of 25 km and overlapping 5 km (detail can be seen in Fig. S1). The Ps phases from the Moho can clearly be seen in the receiver-functions from beneath the western and the eastern flanks of the rift, but are much less clear beneath the rift itself. The arrival time of the Ps-converted phases is about 8.5 s under the eastern flank and about 9 s beneath the western flank of the rift (Fig. 2a and b). Distinctive intra-crustal Ps-converted phases beneath the two flanks of

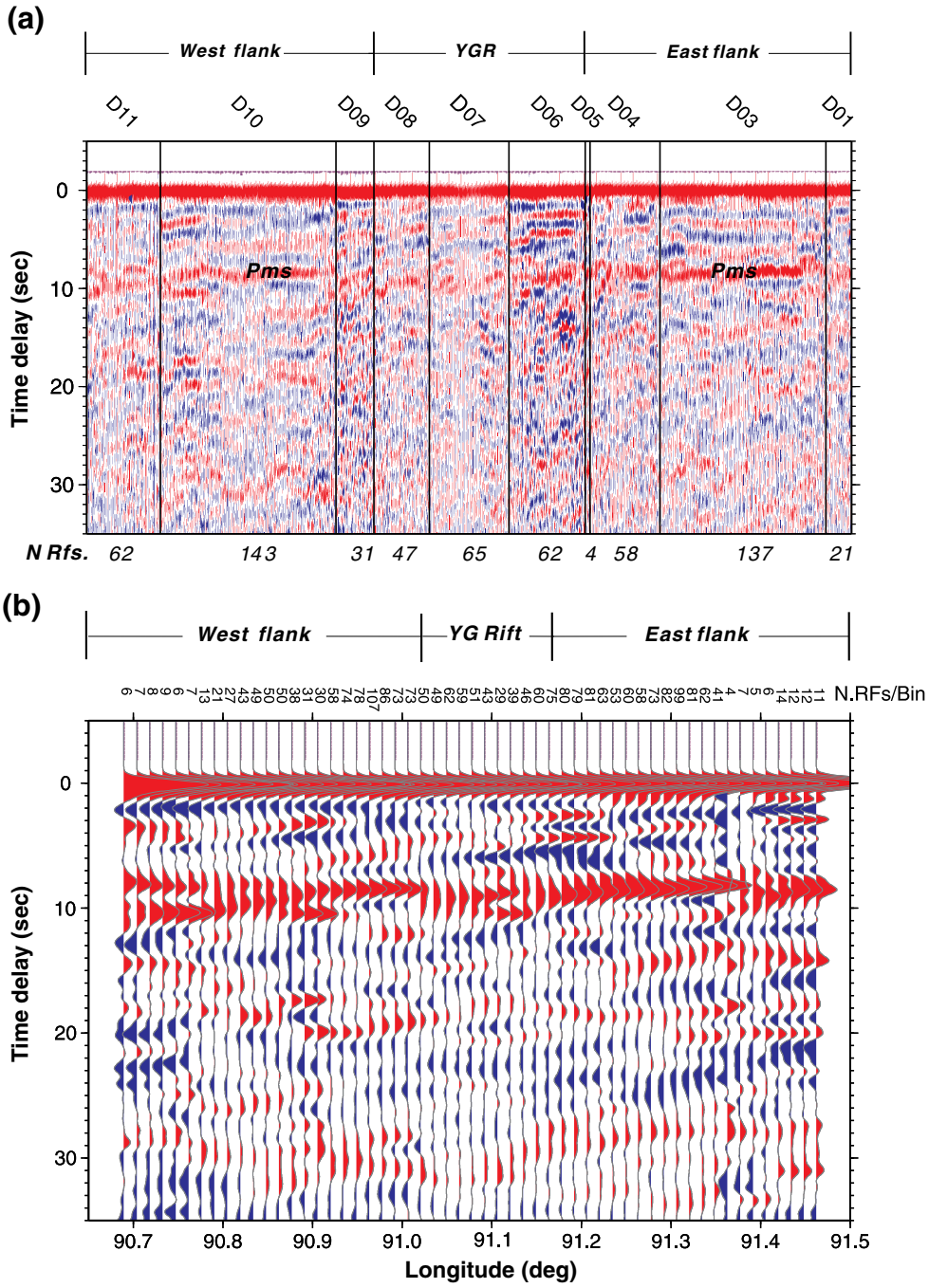

Fig. 2. (a) Raw P-receiver functions for all 11 stations along the profile, grouped by station, sorted by back azimuth and plotted at equal spacing. Red and blue colors are used to indicate the positive and negative amplitudes, respectively. The traces are move-out corrected for each station. The Ps conversion phase of the Moho is also indicated. (b) Stacked P-receiver functions (the summed trace of the move-out corrected receiver function) are for all 11 stations along the profile.

the YGR are apparent. Beneath the YGR and its eastern flank the Moho conversion is stronger and intra-crustal phases are more developed than beneath the western flank. The change in the Moho Ps time and the westward slipping conversion events above the Moho offset beneath the YGR (under stations 6–9) suggests a seismic structural asymmetry of the crust and lithospheric mantle over the axis of the YGR.

4. Migrated receiver function image across the YGR

Fig. 3 presents the migrated PS receiver function section to a depth of 150 km along the profile, using the method of Kind et al. (2002) and the IASP91 model (Kennett and Engdahl, 1991). Fig. 3 shows a remarkable PS conversion event from the Moho discontinuity, at a depth of about 70 km, which is consistent with previous deep seismic soundings (Hirn et al., 1984; Mechie et al., 2012; Min and Wu, 1987; Teng et al., 1981; Zhang and Klemperer, 2005; Zhang et al., 2011) and receiver function results (Kind et al., 2002; Yuan et al., 1997). The structure of the crust and upper mantle can be further supported using a comparison among the migrated Ps, PpPs and PpSs receiver functions (Kind et al., 2002; Fig. S2).

Beneath the eastern flank of the YGR, there is one positive conversion phase at the Moho depth of about 70 km (Fig. 3a). In contrast, beneath the rift and western flank, two strong positive phases are present, which were previously interpreted as a duplex Moho (Kind et al., 2002; Li et al., 2011; Nabelek et al., 2009; Vergne et al., 2002). The shallower one, at a depth of about 75 km, is consistent with the Sino-French west–east profile in the northern Lhasa terrane (Hirn et al., 1984; Min and Wu, 1987; Zhang and Klemperer, 2005), the deeper one occurs at a depth of about 90 km.

5. Crustal Vp/Vs ratio across the YGR

In addition, it is possible to estimate the local depth and average Vp/Vs ratio between the surface and the discontinuity associated with each phase (e.g. Zandt and Ammon, 1995) by measuring the time moveout of the direct converted and reverberated receiver function phases (assuming a locally flat layered structure). We estimated the average crustal Vp/Vs ratio using the H-K stacking method at each station by stacking the receiver function amplitudes at the predicted direct converted phase (Ps) times and reverberated phase (PpPs and PpSs + PsPs) times for several receiver functions over a range of H and Vp/Vs ratio in the H-K domain (Zhu and Kanamori, 2000). The details of the H-K stacking under 11 stations are given in Fig. S3. The result and the trade-off between the Moho depth and the crustal Vp/Vs ratio can be seen in Fig. 4.

Fig. 4 shows the very low Vp/Vs ratio of the crust (about 1.70) along the central segment of the profile, in addition to the lateral variation in the depth of the Moho (about 75 km beneath the rift and western flank and about 70 km beneath the eastern flank). These results suggest that the crustal composition is more felsic than the global average (Christensen and Mooney, 1995). This low average crustal Vp/Vs value is consistent with the crustal Vp/Vs ratio for different tectonic blocks in the Tibetan Plateau, as summarized by Mechie et al. (2012).

6. Discussion and conclusions

6.1. Asymmetry in intracrustal conversion and Vp/Vs ratio across the YGR

Figs. 3 and 4 show three remarkable asymmetrical characteristics of crustal properties across the YGR: (1) shallowing of the Moho and lowering of the average crustal Vp/Vs ratio from the western to the eastern flank of the YGR; (2) stronger crustal conversions beneath the eastern than the western flank of the YGR and (3) one positive Moho conversion phase (Fig. 3) beneath the eastern flank of the YGR, and a duplex Moho with two strong positive phases occurring beneath the rift and western flank. Moho duplex is also observed in the north–south seismic sections (in Hi-climb, INDEPTH and GEDEPTH programs) (Kind et al.,

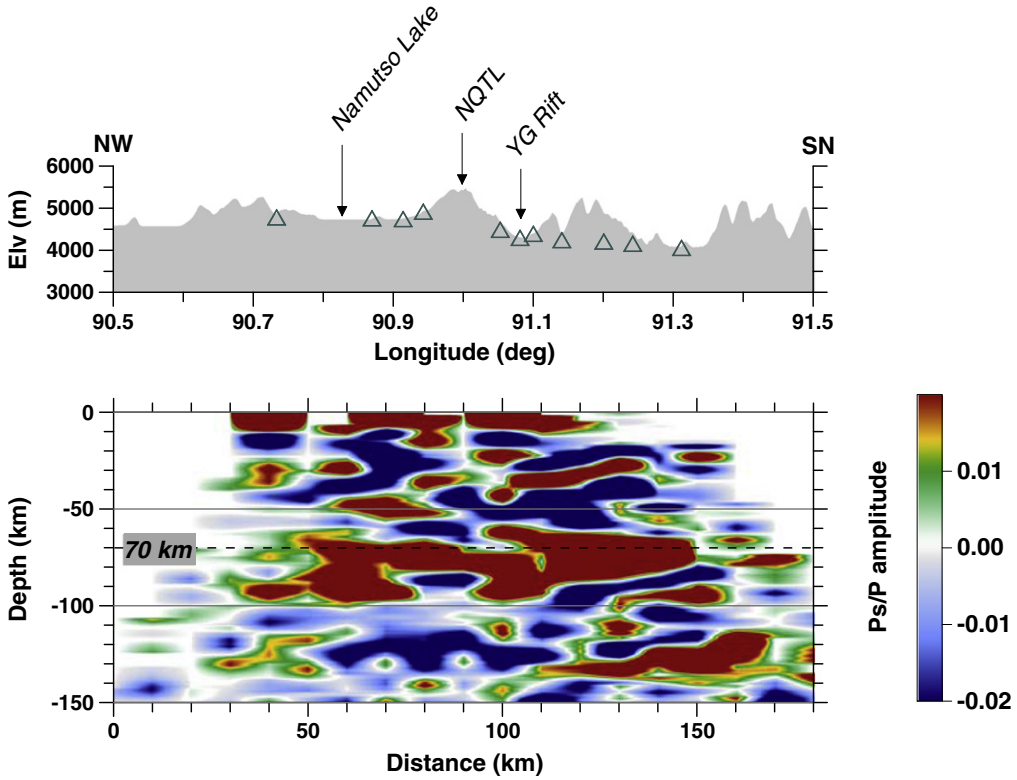

Fig. 3. Migrated Ps wave receiver function images along the profile. Reddish colors indicate positive (velocity increasing downwards) and bluish negative (velocity decreasing downwards) signals.

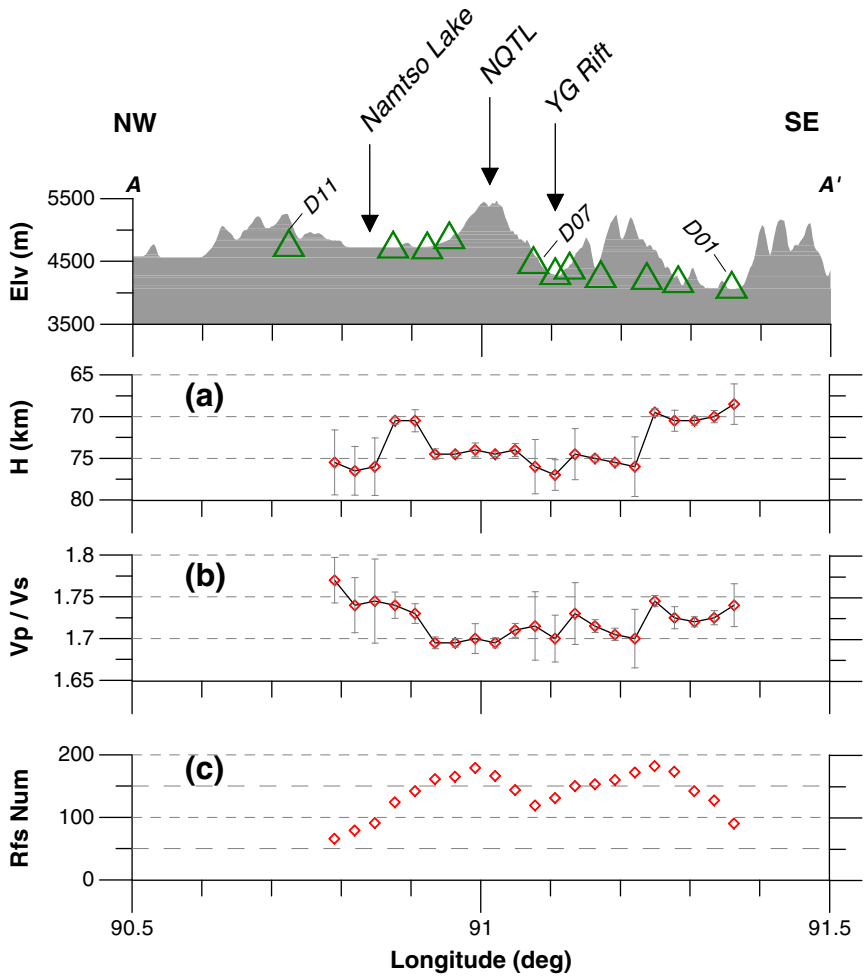

Fig. 4. Crustal thickness and average Vp/Vs ratio along the profile across the Yadong-Gulu Rift.

2002; Nabelek et al., 2009; Vergne et al., 2002) and the deeper Moho is interpreted to represent the bottom of the injected Indian lower crust (Vergne et al., 2002). The 15-km-thick layer between the duplex Moho in the southern Lhasa Block is interpreted to represent the eclogitized or underplated lower crust of India (Nabelek et al., 2009). Klemperer (1987) observed a close relationship between the crustal temperature field and the development of intracrustal reflection. We suggest that this relationship should also be valid in the interpretation of PS conversion in the crust and upper mantle. The difference in the crustal conversion phases across the YGR can be explained by the temperature variation.

Analysis of global deep seismic reflection profiles has shown that the seismic reflectivity is generally stronger in a higher-temperature crust (Klemperer, 1987). Here, we infer that the asymmetry in the intracrustal conversion pattern and the Vp/Vs ratio of the crust is the result of lateral variation in the geothermal field beneath the YGR. The temperature in the crust of the western flank should be lower than beneath the eastern flank. In the YGR, the few existing geothermal measurements (Wei and Deng, 1989) indicate that along our profile, the temperature distribution of the crust and lithospheric mantle shows a clear lateral increase in heat flow from 140 mW/m^2 beneath the western flank to 181 mW/m^2 beneath the Yangbajin (Teng et al., 2004), which is consistent with the low electrical resistance beneath the eastern margin of the rift found in two MT profiles in South Tibet (Wei et al., 2010).

The lateral crustal temperature variation (indicated by the geothermal field and the electric resistance distribution), is consistent with our observation of strong and well developed crustal convertors beneath the rift and its eastern flank (Figs. 2a, b, 3 and 4). The relatively lower temperature beneath the western flank helps to increase the density of the thickened lower crust, and eclogitized the part between the duplex Moho. Here we suggest that the Moho duplex-confined layer is the felsic granulite layer transformed from eclogite. Beneath the eastern flank, no duplex Moho is observed, which can be explained by the eclogitized lower crust being delaminated (Ren and Shen, 2008) or by the lower crust not being eclogitized. This distinctive difference in the Moho conversion pattern between the western and the eastern flanks of the YGR may provide unique information for understanding the transition conditions (including temperature) for the lower crustal eclogitization or delamination.

We observe negative phases in the crust, which indicates a marked variation in the spatial distribution of low velocity layers across the YGR. Beneath the rift and its eastern flank we observe an easterly dipping low velocity channel at a depth of 20–30 km bounded by negative and positive converters. This low velocity zone has also been observed in the INDEPTH profile (Kind et al., 1996; Yuan et al., 1997), and possibly involves fluids and/or partial melting (Makovsky et al., 1996; Nelson et al., 1996). The zone could have resulted from intrusion of magma through the approximately 5-km Moho offset (Fig. 3) beneath the rift and supports the observation of a two-peak geochemical anomaly, with corresponding heat resources from crust and mantle (Ding et al., 2005, 2007). The existence of a lower velocity layer beneath the rift and its eastern flank would attenuate seismic reflection, and can provide an excellent explanation

for the lack of signal beneath the middle crust in the controlled source seismic data of the INDEPTH-II program (Makovsky et al., 1996; Nelson et al., 1996). Beneath the western flank of the rift, there are only a few scattered negative phases. The spatial distribution of the lower velocity layer suggests a complicated magma migration resulting from partial melting generated by simple shear extension beneath the narrow YGR with slip >30°, and a lack of partial melting being generated by the fault with slip <30° (Buck et al., 1988).

6.2. Flesic granulite lower crust and its attributes to asymmetrical structure of the YGR

Even though the lower crust has a high P wave velocity of 7.2–7.5 km/s (Zhang and Klemperer, 2005), our observation of a low crustal Vp/Vs ratio beneath the YGR differs from that for other continental rifts. Most continental rifts have higher values of Vp, Vs and Vp/Vs ratio, indicating alteration of the lower crust. This is the case in most rifting regions, for example the East African Rift (Dugda et al., 2005), Iceland Rift (Darbyshire et al., 2000) and Rio Grande Rift (Mooney et al., 1983; Wilson et al., 2005) (Fig. S4a, b). The high Vp and low Vp/Vs ratio, such as in Kachchh Rift (Mandal, 2011), Baikal Rift (Nielsen and Thybo, 2009) and Rhine Graben (Geissler et al., 2008; Gutscher, 1995), may suggest that felsic granulite, which is rich in quartz (Christensen and Mooney, 1995), may make up most of the lower crust beneath the YGR. The felsic granulitic composition of the lower continental crust beneath the YGR contrasts with the more mafic lower crustal composition estimated in other rifting regions. This suggests a non-underplated crust (Vergne et al., 2008) with regard to the non-linear relationship between crustal thickness and average crustal Vp/Vs ratio (Fig. 4), but is more likely to have resulted from a phase transition in the lower crust (Richardson and England, 1979). In this phase transition process, the early stages of mountain building cause a relatively colder geotherm than would be the case in a thickened crust resulting from the injection of the Indian lower crust (Kind et al., 2002; Nabelek et al., 2009; Owens and Zandt, 1997; Vergne et al., 2002; Zhao et al., 2010). This thermal regime favors the eclogitization of the base of the crust. If, as proposed for the Norwegian Caledonides (Andersen et al., 1991; Dewey et al., 1993), the orogen is immediately followed by a major extensional event, large volumes of crustal eclogites can be brought back to the surface. However, if the crust stays in its thickened state for several tens of millions of years, the temperature increases (with magma intrusion from the asthenosphere through the LAB offset) and the rocks re-equilibrate within the granulite facies in the lower crust as the thickened crust equilibrates thermally (Richardson and England, 1979). This phase transition (eclogite to granulite) at the bottom of the lower crust, which is evidenced by our inferred felsic granulitic composition in the lower crust, led to increased crustal buoyancy, which rapidly uplifted the surface to form the asymmetrical YGR, as observed within the Variscan granulites of the French Massif Central (Mercier et al., 1987; Pin and Vielzeuf, 1983). Our result of a lower average crustal Vp/Vs ratio beneath the YGR excludes the possibility that lithosphere-scale rifts and extension are formed by lower crustal underplating (Nabelek et al., 2009).

6.3. Evaluation of the tectonic mechanism of the normal faulting in South Tibet

A number of mechanisms have been proposed as the cause of the normal faulting. These are: (1) orogenic gravitational collapse (Kapp and Guynn, 2004; Liu and Yang, 2003); (2) middle/lower crustal flow (Royden et al., 2008); (3) shearing from a series of west–east trending

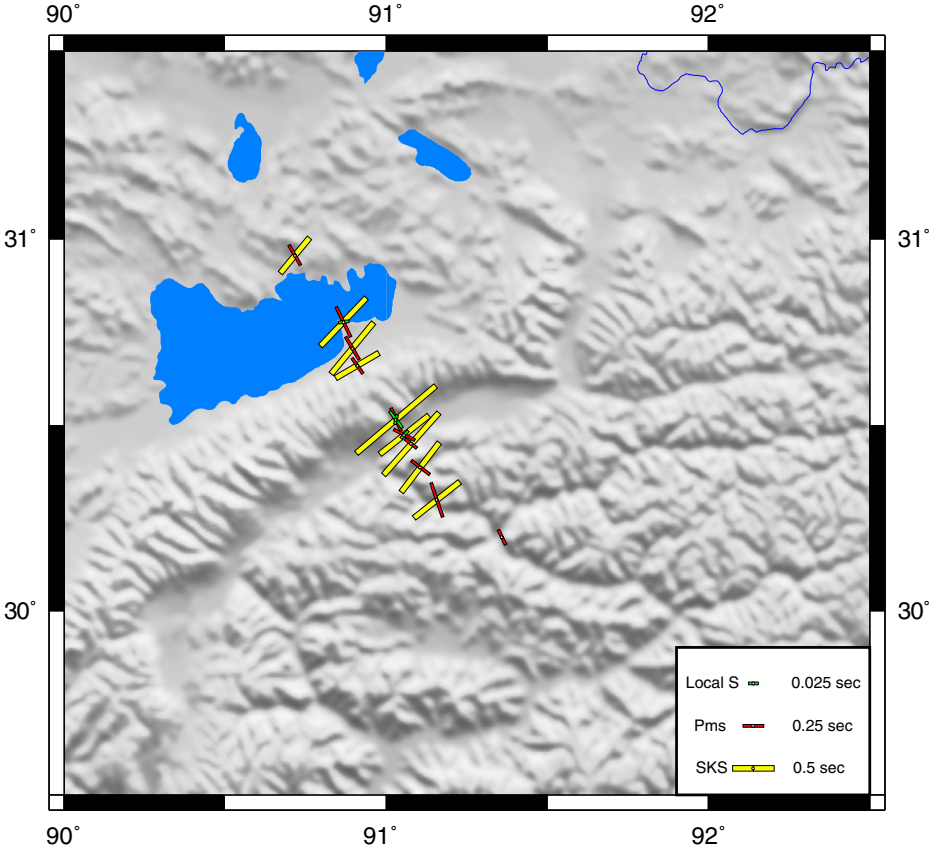

Fig. 5. Polarization direction of the fast-splitting shear wave and delay times between the fast- and slow-splitting shear waves (green: upper crust; red: whole crust from PmS analyses; yellow: SKS).

shear faults (Ratschbacher et al., 2011; Taylor et al., 2003); (4) lithospheric delamination (Houseman and England, 1996); (5) magmatism (Kapp et al., 2005) and (6) lower crustal underplating (Vergne et al., 2008). The orogenic gravitational collapse model is unable to account for the asymmetry of the crustal PS conversion and the low average crustal Vp/Vs ratio. Several characteristics, including asymmetries of topography and heat flow data, suggest that simple shear extension (Buck et al., 1988; Lister et al., 1986; Wernicke, 1981, 1985) is controlling the development of the YGR and lithospheric extension in South Tibet. A simple shear mechanism is an excellent explanation for this asymmetry in the crustal structure.

The asymmetry in the crustal conversion pattern and the low average crustal Vp/Vs ratio leads us to suggest that, in the YGR, simple shear rifting is produced by the eastward flow of the lower crust and mantle lid accommodating the northward injection of Indian lithosphere (Yin and Taylor, 2011). This may suggest that the onset of the north–south normal faulting does not indicate gravitational collapse of the Tibetan lithosphere. Our results don't provide solid evidences to support the gravitational collapse model (Ratschbacher et al., 2011; Taylor et al., 2003). Our present inference about the collapse is that it should be at the early stage if it signatures the gravitational collapse (Buck et al., 1988) as we don't observe remarkable thinning of crust and lithosphere, but only offset of the Moho beneath the YGR. Our crustal structure and the shallow/deep deformation decoupling with inconsistency between shallow (evidenced by PmS shear wave splitting analyses) and deep (evidenced by SKS shear wave splitting measurements) (Fig. 5) across the YGR may provide supports to the transpression mechanism (Ratschbacher et al., 2011; Yin and Taylor, 2011), and the eastward escape model (Klemperer, 2006; Tapponnier et al., 1981; Zhang and Klemperer, 2005) for the lower crust of Lhasa terrane or even whole lithosphere of south Tibet.

In principle, SKS splitting results from strain-induced lattice preferred orientations of anisotropic minerals (such as olivine) in the upper mantle, and represents the orientation of strain or flow in the uppermost mantle. Analysis of Moho converted P to S waves, which sample the crust, provides well-constrained orientations for near-surface and middle crustal anisotropy. To assess the inference made above, we conducted analyses of shear wave splitting, which included SKS splitting analyses and Moho conversions using the same scheme as Chen et al. (2013). Shear wave splitting was analyzed in the upper crust with the direct shear wave (of the local earthquake events) within shear wave window (Gao et al., 2010). Polarization direction of the fast-splitting shear wave and delay times between the fast- and slow-splitting shear waves (green: upper crust; red: whole crust from PmS analyses; yellow: SKS) are shown in Fig. 5. Our results show that the predominant deformation direction from SKS splitting analyses, is consistent in the direction of north–east, which are consistent with the deformation direction from GPS measurements (Gan et al., 2007). A similarity in Surface GPS and SKS shear wave splitting data in South Tibet was also observed in the previous studies (Flesch et al., 2005; Wang et al., 2008). This similarity suggests that the upper crust and upper mantle can exhibit similar horizontal velocity fields, in a coherent deformation as proposed by Flesch et al. (2005). However, our polarization directions from Moho PmS shear

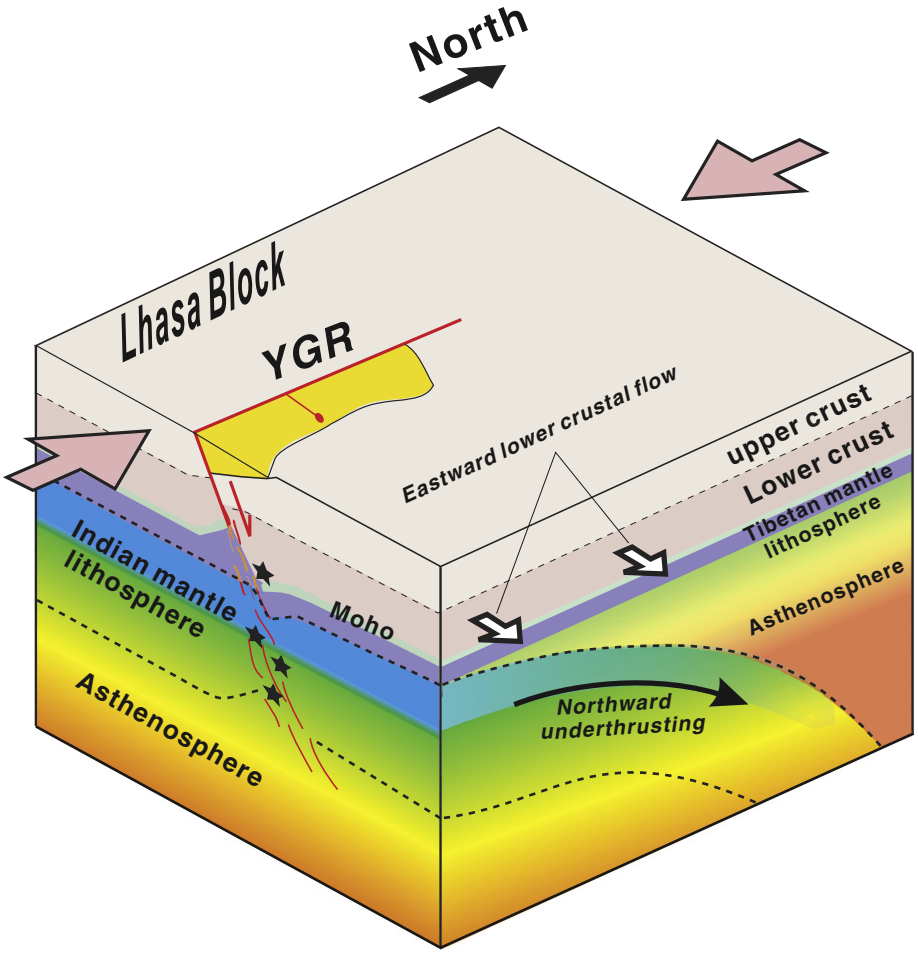

Fig. 6. Cartoon map of the formation of the YGR during north–south shortening between the Indian and Eurasian plates.

wave splitting analyses of the whole crust and direct shear wave splitting study of upper crust, are in the direction of the northwest–southeast (Fig. 5). As delay times between the fast and slow splitting shear waves in the top 10 km of the crust (local earthquake depths of 8–10 km) are less than 0.025 s, much less than the delay time in the whole crust estimated from PmS splitting analyses. Anisotropy is then mainly attributed to the middle/lower crust, and the deformation direction in the lower crust should be in the NW–SE. In this way, there is an obvious inconsistence of deformation direction between the lower crust and lithospheric mantle. This inconsistency leads us to infer that the upper crust and lithospheric mantle are mechanically decoupled by an intermediate weak lower crust or mantle lid, as indicated by a 3-D multilayer modeling of the continental collision (Lechmann et al., 2011) and lithospheric rheology study (Zhang et al., 2013). With the north–south underthrusting of the Indian plate beneath Tibet, lithospheric thickening, and eastward flow in the lower crust and mantle lid to accommodate the north–south shortening (Fig. 6), the viscosity in the lower crust and mantle wedge decreases dramatically with the increase in temperature and fluid inclusion from the subducting slab. This eastward flow as a horizontal shear at the base of upper crust triggers normal faulting by simple shear. Here, we propose that this simple/general shear rifting in the YGR is produced by eastward (horizontal) shear at the base of the upper crust, as evidenced by the observed Tibetan GPS velocity field (Yin and Taylor, 2011), and our observation of the discrepancies in shear wave splitting among the upper crust, lower crust and lithospheric mantle.

In summary, the simple shear model can explain the rapid uplift of the YGR through small-scale convection (Buck et al., 1988) induced in the mantle beneath a rift due to the lateral temperature gradients there. This convection increases the amount of heat transported vertically into the rift and laterally out of it. The mantle flow results in thinning of the adjacent lithosphere causing flanking uplift as well as slowing of the subsidence of the middle of the rift (Fig. 6). The magnitude of the uplift is dependent on the geometry of the rift and the importance of stress-dependence in the rheology of the mantle (Buck et al., 1988). For viscosity parameters which are consistent with the pre-rift temperature structure small-scale convection can produce uplift at least twice as great as would be produced by lateral conduction alone. Lithosphere extension is also probably the manifestation of late stage transpression jointly caused by the Indian plate sliding obliquely beneath Tibet along a gently dipping, arcuate plate boundary (Avouac and Tapponnier, 1993; Dewey, 1988; England and Molnar, 1997; Peltzer and Tapponnier, 1988; Ratschbacher et al., 2011; Taylor et al., 2003; Yin, 2000) or acts as a signature of the west–east extension resulting from a triple junction confined by the BNS fault at its north and Nyainqentanghla-Jiali fault at its south even though our experiment cannot resolve an apparent doming with the high seismic velocity across the YGR. The wide-spread lower velocity layer in the middle crust (Mechie et al., 2012; Zhang et al., 2011) and high geothermal data (Teng et al., 2004) suggest the contribution of magmatism to enhance the north–south rifting (Harrison, 2006).

Supplementary data to this article can be found online at http://dx.doi.org/10.1016/j.tecto.2013.03.019.

Acknowledgments

This study was supported by Sinoprobe-02-03, the National Natural Science Foundation of China (40830315, 41021063), the Chinese Academy of Sciences (KZCX2-YW-132), and the Deutsche Forschungsgemeinschaft. The authors thank the Seismological Experiment Laboratory, IGGCAS for the field data. Profs. Kind, Drs. Nedunchezhiyan and Jolivet and other reviewers are also appreciated for their constructive comments and suggestions to improve the presentation of the paper.

References

Andersen, T.B., Jamtveit, B., Dewey, J.F., Swensson, E., 1991. Subduction and education of continental crust: major mechanisms during continent–continent collision and orogenic extensional collapse, a model based on the south Norwegian Caledonides. Terra Nova 3, 303–310.
Armijo, R., Tapponnier, P., Mercier, J.L., Han, T., 1986. Quaternary extension in southern Tibet: field observations and tectonic implications. Journal of Geophysical Research 91, 13,803–13,872.
Armijo, R., Tapponnier, P., Han, T., 1989. Late Cenozoic right-lateral strike-slip faulting across southern Tibet. Journal of Geophysical Research 94, 2787–2838.
Avouac, J.P., Tapponnier, P., 1993. Kinematic model of active deformation in central Asia. Geophysical Research Letters 20 (10), 895–898.
Buck, R.W., Martinez, F., Steckler, M.S., Cochran, J.R., 1988. Thermal consequences of lithospheric extension: pure and simple. Tectonics 7, 213–234.
Chen, Y., Zhang, Z., Sun, C., Badal, J., 2013. Crustal anisotropy from Moho converted Ps wave splitting analysis and geodynamic implications beneath the eastern margin of Tibet and surrounding regions. Gondwana Research. http://dx.doi.org/10.1016/j.gr.2012.1004.1003.
Christensen, N.I., Mooney, W.D., 1995. Seismic velocity structure and composition of the continental crust: A global view. Journal of Geophysical Research 100, 9761–9788.
Chung, S.L., Chu, M.F., Zhang, Y.Q., Xie, Y.W., Lo, C.H., Lee, T.Y., Lan, C.Y., Li, X.H., Zhang, Q., Wang, Y.H., 2005. Tibetan tectonic evolution inferred from spatial and temporal variations in post-collisional magmatism. Earth-Science Reviews 68, 173–196.
Darbyshire, F.A., Priestley, K.F., White, R.S., et al., 2000. Crustal structure of central and northern Iceland from analysis of teleseismic receiver functions. Geophysical Journal International 143, 163–184.
Dewey, J., 1988. Extensional collapse of orogens. Tectonics 7 (6), 1123–1139.
Dewey, J.F., Burke, K., 1973. Tibetan, Variscan, and Precambrian basement reactivation: products of continental collision. Journal of Geology 81, 683–692.
Dewey, J.F., Ryan, P.D., Andersen, T.B., 1993. Orogenic uplift and collapse, crustal thickness, fabrics and metamorphic changes: the role of eclogites. Geological Society, London, Special Publications 76, 325–343.
Ding, L., Kapp, P., Wan, X.Q., 2005. Paleocene–Eocene record of ophiolite obduction and initial India-Asia collision, south central Tibet. Tectonics 24, TC3001. http://dx.doi.org/10.1029/2004TC001729.
Ding, L., Kapp, P., Yue, Y., Lai, Q., 2007. Postcollisional calc-alkaline lavas and xenoliths from the southern Qiangtang terrane, central Tibet. Earth and Planetary Science Letters 254, 28–38.
Dugda, M.T., Nyblade, A.A., Julia, J., Langston, C.A., Ammon, C.J., Simiyu, S., 2005. Crustal structure in Ethiopia and Kenya from receiver function analysis: implications for rift development in eastern Africa. Journal of Geophysical Research 110, B01303. http://dx.doi.org/10.1029/2004JB003065.
England, P., Molnar, P., 1997. The field of crustal velocity in Asia calculated from Quaternary rates of slip on faults. Geophysical Journal International 130 (3), 551–582.
Flesch, L.M., Holt, W.E., Silver, P.G., Stephenson, M., Wang, C.Y., Chan, W.W., 2005. Constraining the extent of crust-mantle coupling in Central Asia using GPS, geologic, and shear-wave splitting data. Earth and Planetary Science Letters 238, 248–268. http://dx.doi.org/10.1016/j.epsl.2005.06.023.
Gan, W., Zhang, P., Shen, Z.K., Niu, Z., Wang, M., Wan, Y., Zhou, D., Cheng, J., 2007. Present-day crustal motion within the Tibetan Plateau inferred from GPS measurements. Journal of Geophysical Research 112 (B8), B08416.
Gao, Y., Wu, J., Yi, G.X., Shi, Y.T., 2010. Crust-mantle coupling in North China: preliminary analysis from seismic anisotropy. Chinese Science Bulletin 55. http://dx.doi.org/10.1007/s11434-010-4135-y.
Geissler, W.H., Kind, R., Yuan, X., 2008. Upper mantle and lithospheric heterogeneities in central and eastern Europe as observed by teleseismic receiver function. Geophysical Journal International 174, 351–376.
Gutscher, M., 1995. Crustal structure and dynamics in the Rhine Graben and the Alpine foreland. Geophysical Journal International 122, 617–636.
Harrison, T.M., 2006. Did the Himalayan Crystallines extrude partially molten from beneath the Tibetan Plateau? Geological Society, London, Special Publications 268 (1), 237–254.
Harrison, T.M., Copeland, P., Kidd, W.S.F., Lovera, O.M., 1995. Activation of the Nyainqentanghla shear zone: implications for uplift of the southern Tibetan plateau. Tectonics 14, 658–676.
Hirn, A., Lepine, J., Jobert, G., Sapin, M., Wittlinger, G., Xu, Z.Q., Gao, E.Y., Wang, X.J., Teng, J.W., Xiong, S.B., Pandey, M.R., Tater, J.M., 1984. Crustal structure and variability of the Himalayan border of Tibet. Nature 307, 23–25.
Houseman, G., England, P.C., 1996. A lithospheric thickening model for the Indo-Asian collision. In: Yin, A., Harrison, T.M. (Eds.), Tectonic Evolution of Asia. Cambridge University Press, New York, pp. 3–17.
Kapp, P., Guynn, J.H., 2004. Indian punch rifts Tibet. Geology 32, 993–996.
Kapp, J.L.D., Harrison, T.M., Kapp, P., Grove, M., Lovera, O.M., Lin, D., 2005. Nyainqentanglha Shan: a window into the tectonic, thermal, and geochemical evolution of the Lhasa block, southern Tibet. Journal of Geophysical Research 110, B08413. http://dx.doi.org/10.1029/2004JB003330.
Kapp, P., Taylor, M., Stockli, D., Ding, L., 2008. Development of active low-angle normal fault systems during orogenic collapse: insight from Tibet. Geology 36, 7–10.
Kennett, B.L.N., Engdahl, E.R., 1991. Traveltimes for global earthquake location and phase identification. Geophysical Journal International 105, 429–465.
Kind, R., Ni, J., Zhao, W., Wu, J., Yuan, X., Zhao, L., Sandvol, E., Reese, C., Nabelek, J., Hearn, T., 1996. Evidence from earthquake data for a partially molten crustal layer in southern Tibet. Science 274, 1692–1694.
Kind, R., Yuan, X., Saul, J., Nelson, D., Sobolev, S., Mechie, J., Zhao, W., Kosarev, G., Ni, J., Achauer, U., 2002. Seismic images of crust and upper mantle beneath Tibet:

evidence for Eurasian plate subduction. Science 298, 1219–1221. http://dx.doi.org/10.1126/science.1078115.
Kind, R., Yuan, X., Kumar, P., 2012. Seismic receiver functions and the lithosphere–asthenosphere boundary. Tectonophysics 536–537, 25–43.
Klemperer, S.L., 1987. A relation between continental heat flow and the seismic reflectivity of the lower crust. Journal of Geophysical Research 61, 1–11.
Klemperer, S.L., 2006. Crustal flow in Tibet: geophysical evidence for the physical state of Tibetan lithosphere, and inferred patterns of active flow. Geological Society, London, Special Publications 268 (1), 39–70.
Larson, K.M., Burgmann, R., Bilham, R., Freymueller, J.T., 1999. Kinematics of the India-Eurasia collision zone from GPS measurements. Journal of Geophysical Research 104, 1077–1093. http://dx.doi.org/10.1029/1998JB900043.
Lechmann, S.M., May, D.A., Kaus, B.J.P., Schmalholz, S.M., 2011. Comparing thin-sheet models with 3-D multilayer models for continental collision. Geophysical Journal International 187, 10–33.
Li, X., Wei, D., Yuan, X., Kind, R., Kumar, P., Zhou, H., 2011. Details of the doublet Moho structure beneath Lhasa, Tibet, obtained by comparison of P and S receiver functions. Bulletin of the Seismological Society of America 101 (3), 1259–1269.
Ligorria, J.P., Ammon, C.J., 1999. Iterative deconvolution and receiver-function estimation. Bulletin of the Seismological Society of America 89, 1395–1400.
Lister, G.S., Etheridge, M.A., Symonds, P.A., 1986. Application of the detachment fault model to the formation of passive continental margins. Geology 14, 246–250.
Liu, M., Yang, Y., 2003. Extensional collapse of the Tibetan Plateau: results of three-dimensional finite element modeling. Journal of Geophysical Research 108 (B8), 2361.
Maheo, G., Leloup, P.H., Valli, F., Lacassin, R., Arnaud, N., Paquette, J.L., Fernandez, A., Haibing, L., Farley, K.A., Tapponnier, P., 2007. Post 4 Ma initiation of normal faulting in southern Tibet. Constraints from the Kung Co half graben. Earth and Planetary Science Letters 256 (1–2), 233–243. http://dx.doi.org/10.1016/j.epsl.2007.01.029.
Makovsky, Y., Klemperer, S.L., Huang, L.-Y., Lu, D.-Y., TEAM Project INDEPTH, 1996. Structural elements of the southern Tethyan Himalaya crust from wide-angle seismic data. Tectonics 15, 997–1005.
Mandal, P., 2011. Upper mantle seismic anisotropy in the intra-continental Kachchh rift zone, Gujarat, India. Tectonophysics 509, 81–92.
McCaffrey, R., Nabelek, J., 1998. Role of oblique convergence in the active deformation of the Himalayas and southern Tibet plateau. Geology 26, 691–694.
Mechie, J., Zhao, W., Karplus, M., Wu, Z., Meissner, R., Shi, D., Klemperer, S., Su, H., Kind, R., Xue, G., 2012. Crustal shear (S) velocity and Poisson's ratio structure along the INDEPTH IV profile in northeast Tibet as derived from wide-angle seismic data. Geophysical Journal International 191 (2), 369–384.
Mercier, J.-L., Armijo, R., Tapponnier, P., Carey-Gailhardis, E., Han, T., 1987. Change from Tertiary compression to Quaternary extension in southern Tibet during the India-Asia collision. Tectonics 6, 275–304.
Min, Z., Wu, F.T., 1987. Nature of the upper crust beneath central Tibet. Earth and Planetary Science Letters 84, 204–210.
Molnar, P., Tapponnier, P., 1978. Active tectonics of Tibet. Journal of Geophysical Research 83, 5361–5375. http://dx.doi.org/10.1029/JB083iB11p05361.
Mooney, W., Andrews, M., Ginzburg, A., Peters, D., Hamilton, R., 1983. Crustal structure of the northern Mississippi embayment and a comparison with other continental rift zones. Tectonophysics 94, 327–348.
Nabelek, J., Hetenyi, G., Vergne, J., Sapkota, S., Kafle, B., Jiang, M., Su, H., Chen, J., Huang, B.-S., the Hi-CLIMB Team, 2009. Underplating in the Himalaya–Tibet collision zone revealed by the Hi-CLIMB experiment. Science 325, 1371–1374. http://dx.doi.org/10.1126/science.1167719.
Nelson, K.D., Zhao, W., Brown, L., Kuo, J., Che, J., Liu, X., Klemperer, S., Makovsky, Y., Meissner, R., Mechie, J., 1996. Partially molten middle crust beneath southern Tibet: synthesis of project INDEPTH results. Science 274, 1684–1688.
Nielsen, C., Thybo, H., 2009. Lower crustal intrusions beneath the southern Baikal Rift Zone: evidence from full-waveform modeling of wide angle seismic data. Tectonophysics 470, 298–318.
Owens, T.J., Zandt, G., 1997. Implications of crustal property variations for models of Tibetan Plateau evolution. Nature 387, 37–43.
Peltzer, G., Tapponnier, P., 1988. Formation and evolution of strike-slip faults, rifts, and basins during the India-Asia collision: an experimental approach. Journal of Geophysical Research 93, 15085–15117.
Pin, G., Vielzeuf, D., 1983. Cranulites and related rocks in Variscan median Europe: a dualistic interpretation. Tectonophysics 93, 47–74.
Ratschbacher, L., Krumeri, I., Blumenwitz, M., Staiger, M., Gloaguen, R., Miller, B.V., Samson, S.D., Edwards, M.A., Appel, E., 2011. Rifting and strike-slip shear in central Tibet and the geometry, age and kinematics of upper crustal extension in Tibet. In: Gloaguen, R., Ratschbacher, L. (Eds.), Growth and Collapse of the Tibetan Plateau: Geological Society, London, Special Publications, 253, pp. 127–163.
Ren, Y., Shen, Y., 2008. Finite frequency tomography in southeastern Tibet: evidence for the causal relationship between mantle lithosphere delamination and the north–south trending rifts. Journal of Geophysical Research 113, B10316. http://dx.doi.org/10.1029/2008JB005615.
Richardson, S.W., England, P.C., 1979. Metamorphic consequences of crustal eclogite production in overthrust orogenic zones. Earth and Planetary Science Letters 42, 183–190.
Royden, L.H., Burchfiel, B.C., van der Hilst, R.D., 2008. The geological evolution of the Tibetan Plateau. Science 321, 1054. http://dx.doi.org/10.1126/science.1155371.
Shapiro, N.M., Ritzwoller, M.H., Molnar, P., Levin, V., 2004. Thinning and flow of Tibetan crust constrained by seismic anisotropy. Science 305 (5681), 233–236.
Tapponnier, P., Mercier, J.L., Armijo, R., Han, T., Zhao, J., 1981. Field evidence for active normal faulting in Tibet. Nature 294, 410–414. http://dx.doi.org/10.1038/294410a0.
Taylor, M., Yin, A., Ryerson, F.J., Kapp, P., Ding, L., 2003. Conjugate strike-slip faulting along the Bangong–Nujiang suture zone accommodates coeval east–west extension and north-south shortening in the interior of the Tibetan Plateau. Tectonics 22 (4), 1044. http://dx.doi.org/10.1029/2002TC001361.
Teng, J.W., Xiong, S.B., Sun, K.Z., 1981. Explosive seismology for crust and upper mantle structure and velocity distribution beneath Danxiong–Yadong areas, Xizang Plateau. Chinese Journal of Geophysics (Chinese Edition) 24 (2), 155–170.
Teng, J.W., Zhang, Z.J., Bai, W.M., 2004. Physics of Lithosphere. Science Press, Beijing (in Chinese).
Vergne, J., Wittlinger, G., Hui, Q., Tapponnier, P., Poupinet, G., Mei, J., Herquel, G., Paul, A., 2002. Seismic evidence for stepwise thickening of the crust across the NE Tibetan plateau. Earth and Planetary Science Letters 203, 25–33.
Vergne, J., Cattin, R., Avouac, J., 2008. On the use of dislocations to model interseismic strain and stress build-up at intracontinental thrust faults. Geophysical Journal International 147 (1), 155–162.
Wang, C.Y., Flesch, L.M., Silver, P.G., Chang, L.J., Chan, W.W., 2008. Evidence for mechanically coupled lithosphere in central Asia and resulting implications. Geology 36 (5), 363–366.
Wei, S.Y., Deng, X.Y., 1989. Geothermal activity, geophysical anomalies and the geothermal state of the crust and upper mantle in the Yarlung Zangbo river zone. Tectonophysics 159, 247–254.
Wei, W.B., Jin, S., Ye, G.F., Deng, M., Jing, J.E., Unsworth, M., Jones, A.G., 2010. Conductivity structure and rheological property of lithosphere in Southern Tibet inferred from super-broadband magnetotelluric sounding. Science China Earth Sciences 53 (2), 189–202.
Wernicke, B., 1981. Low-angle normal faults in the Basin and Range Province: nappe tectonics in an extending orogen. Nature 291, 645–648.
Wernicke, B., 1985. Uniform-sense normal simple shear of the continental lithosphere. Canadian Journal of Earth Sciences 22, 108–125.
Wilson, D., Aster, R., Ni, J., 2005. Imaging the seismic structure of the crust and upper mantle beneath the Great Plains, Rio Grande Rift, and Colorado Plateau using receiver functions. Journal of Geophysical Research 110, B05306. http://dx.doi.org/10.1029/2004JB003492.
Yin, A., 2000. Mode of Cenozoic east–west extension in Tibet suggesting a common origin of rifts in Asia during the Indo-Asian collision. Journal of Geophysical Research 105, 21,745–21,759. http://dx.doi.org/10.1029/2000JB900168.
Yin, A., Harrison, T.M., 2000. Geologic evolution of the Himalayan–Tibetan orogen. Annual Review of Earth and Planetary Sciences 28, 211–280.
Yin, A., Taylor, M.H., 2011. Mechanics of V-shaped conjugate strike-slip faults and the corresponding continuum model of continental deformation. GSA Bulletin 123 (9–10), 1798–1821.
Yuan, X., Ni, J., Kind, R., Mechie, J., Sandvol, E., 1997. Lithospheric and upper mantle structure of southern Tibet from a seismological passive source experiment. Journal of Geophysical Research 102, 27491–27500.
Zandt, G., Ammon, C.J., 1995. Continental crust composition constrained by measurements of crustal Poisson's ratio. Nature 374 (6518), 152–154.
Zhang, Z., Klemperer, S.L., 2005. West–east variation in crustal thickness in northern Lhasa block, central Tibet, from deep seismic sounding data. Journal of Geophysical Research 110, B09403. http://dx.doi.org/10.1029/2004JB003139.
Zhang, Z., Deng, Y., Teng, J., Wang, C., Gao, R., Chen, Y., Fan, W., 2011. An overview of the crustal structure of the Tibetan plateau after 35 years of deep seismic soundings. Journal of Asian Earth Sciences 40 (4), 977–989.
Zhang, Z., Deng, Y., Chen, L., Wu, J., Teng, J.W., Panza, G.F., 2013. Seismic structure and rheology of the crust under mainland China. Gondwana Research. http://dx.doi.org/10.1016/j.gr.2012.07.010.
Zhao, W.J., Nelson, K.D., Project INDEPTH Team, 1993. Deep seismic reflection evidence for continental underthrusting beneath southern Tibet. Nature 366, 557–559.
Zhao, J., Yuan, X., Liu, H., Kumar, P., Pei, S., Kind, R., Zhang, Z., Teng, J., Ding, L., Gao, X., Xu, Q., Wang, W., 2010. The boundary between the Indian and Asian tectonic plates below Tibet. Proceedings of the National Academy of Sciences of the United States of America 107, 11229–11233.
Zhu, L., Kanamori, H., 2000. Moho depth variation in southern California from teleseismic receiver functions. Journal of Geophysical Research 105, 2969–2980.